

Collective dynamics of fermion clouds in cigar-shaped traps

Z. Akdeniz^{a,b}, P. Vignolo^a and M.P. Tosi^{a,*}

^a*NEST-INFM and Classe di Scienze, Scuola Normale Superiore,
I-56126 Pisa, Italy*

^b*Department of Physics, University of Istanbul, Istanbul, Turkey*

Abstract

The propagation of zero sound in a spin-polarized Fermi gas under harmonic confinement is studied as a function of the mean-field interactions with a second Fermi gas. A local-density treatment is compared with the numerical solution of the Vlasov-Landau equations for the propagation of density distortions in a trapped two-component Fermi gas at temperature $T = 0.2T_F$. The response of the gas to the sudden creation of a sharp hole at its centre is also studied numerically.

Key words: Fermi gases, zero sound

PACS: 03.75.Ss, 05.30.Fk

1 Introduction

Current experiments on the collisional properties of a Fermi gas in two spin-polarized states under confinement have proven that this setup provides an important tool for investigating the dynamics of dilute quantum gases. For such a system in harmonic trapping the existence of zero and first sound excitations has been demonstrated experimentally [1,2] and numerically [3] by measuring the damping of the oscillations of a non-equilibrium density profile as a function of the collision rate. These studies have followed the evolution of the dynamical behaviour of the quantum gas from a collisional (first sound) regime to a collisionless (zero sound) regime. However, no direct measurement of the speed of sound propagation has been carried out so far in confined Fermi gases, contrary to the case of Bose-Einstein condensates in elongated traps [4] where the propagation of density distortions has been followed experimentally.

* Corresponding author, e-mail: tosim@sns.it

The main purpose of the present study is to evaluate by both theoretical and numerical means the propagation of density distortions in the zero-sound regime for a degenerate Fermi gas contained inside a cigar-shaped harmonic trap, in situations that are accessible to experiment. It may be useful to recall at this point the earlier studies of these collective excitations in homogeneous Fermi fluids. The experiments of Abel *et al.* [5] on acoustic waves propagating through liquid ^3He demonstrated that the transition from collisional to collisionless dynamics is signalled by a drastic change in the frequency dependence of sound-wave attenuation and showed that the difference in the speeds of first and zero sound is quite small. This is as expected for a strongly coupled Fermi liquid from the Landau theory [6]. The evolution of the zero-sound dispersion relation in liquid ^3He into the microscopic regime was determined by Sköld *et al.* [7] in inelastic neutron scattering experiments and accounted for theoretically by Aldrich *et al.* [8] within a polarization potential approach extending Landau's Fermi-liquid theory to larger momenta and energies. Landau's theory has also been used by Yip and Ho [9] to evaluate the collisionless excitation modes corresponding to density fluctuations and to coherent interconversion of various spin species in a homogeneous Fermi gas.

At variance from the strongly coupled ^3He liquid, in a dilute Fermi gas the interactions can be expected to introduce only slight modifications to the bare sound velocities, which in the homogeneous noninteracting limit are v_F and $v_F/\sqrt{3}$ for zero and first sound, respectively. Here, the Fermi velocity v_F is determined by the Fermi wave number and hence by the particle number density. These well-known results [6] immediately suggest how the propagation of collective density fluctuations in a confined Fermi gas may be treated within a local-density approximation.

In this work we first present an analytical study of the behaviour of the Fermi velocity and of the speed of zero sound in a two-component inhomogeneous Fermi gas as functions of the mean-field interactions in the collisionless regime. We support our analytical estimate by numerical simulations solving the Vlasov-Landau equations (VLE) for the fermionic Wigner distributions at $T = 0.2T_F$, T_F being the Fermi temperature [3]. We evaluate the propagation of zero sound by simulating an experiment where perturbation in the density profile is introduced by a laser beam permanently focused on the centre of the trap [10,11]. We also simulate an experiment carried on by Dutton *et al.* [12] on a Bose-Einstein condensate, where a defect with a large gradient in the density is generated by cutting off a slice of the profile by means of an ultra-compressed slow pulse of light. In their experiment the generation of quantum shock waves in the condensate was observed.

The paper is organized as follows. In Sec. 2 we recall the equations of motion for a two-component Fermi gas and evaluate in a semiclassical local-density approach the Fermi velocity and the zero sound velocity for such a system. In

Sec. 3 we report illustrations of our numerical simulations for a one-component and a two-component Fermi gas, and compare the results with our theoretical estimates. Conclusions and perspectives are given in Sec. 4.

2 The model

The two spin-polarized fermionic components of the gas are described by the Wigner distribution functions $f^{(j)}(\mathbf{r}, \mathbf{p}, t)$, with $j = 1$ or 2 . These obey the kinetic equations

$$\frac{\partial f^{(j)}}{\partial t} + \frac{\mathbf{p}}{m_j} \cdot \nabla f^{(j)} - \nabla U^{(j)} \cdot \nabla_{\mathbf{p}} f^{(j)} = C_{12}[f^{(j)}]. \quad (1)$$

At high dilution the interactions between atoms of the same spin are suppressed by the Pauli principle, so that the mean-field Hartree-Fock (HF) effective potentials are $U^{(j)}(\mathbf{r}, t) = V_{ext}^{(j)}(\mathbf{r}, t) + gn^{(\bar{j})}(\mathbf{r}, t)$ with \bar{j} indicating the species different from j and $V_{ext}^{(j)}(\mathbf{r}, t)$ being the sum of external confining and driving potentials. Here we have set $\hbar = 1$ and $g = 2\pi a/m_r$, with a the s -wave scattering length ($a > 0$ for the present case of repulsive interactions) and m_r the reduced mass. The total spatial densities $n^{(j)}(\mathbf{r}, t) = n_0^{(j)}(\mathbf{r}) + \delta n^{(j)}(\mathbf{r}, t)$ are the sum of the equilibrium densities $n_0^{(j)}(\mathbf{r})$ and the time-dependent perturbations $\delta n^{(j)}(\mathbf{r}, t)$, and are obtained by integration of $f^{(j)}(\mathbf{r}, \mathbf{p}, t)$ in momentum space. Finally $C_{12}[f^{(j)}]$ is the collision integral, which will be set to zero in the collisionless regime. Equation (1) in this regime will be solved numerically in Sec. 3, using the algorithm developed by Toschi *et al.* [3] and taking the equilibrium density profiles as given in the HF approach [13] by

$$n_0^{(j)}(\mathbf{r}) = \int \frac{d^3p}{(2\pi)^3} \left\{ \exp \left[\beta \left(\frac{p^2}{2m_j} + U^{(j)}(\mathbf{r}) - \mu^{(j)} \right) \right] + 1 \right\}^{-1}, \quad (2)$$

where $\beta = 1/k_B T$ and $\mu^{(j)}$ is the chemical potential of species j .

In the rest of this section we present instead a theoretical discussion of the long-wavelength excitations of the gas. The perturbation $\delta n^{(j)}(\mathbf{r}, t)$ moves with a group velocity whose natural unit is the Fermi velocity $v_F^{(j)}$. In an inhomogeneous gas the Fermi velocities depend on position and will be related below to the local chemical potential of each species through a local density approximation. Assuming for the moment that they are known, the dynamical response of the two-component Fermi gas can be calculated within a random phase approximation [14,15] from the set of eigenvalue equations

$$\delta n^{(j)}(q, \Omega) = -\chi_j(q, \Omega) [\delta V^{(j)}(q, \Omega) + g\delta n^{(\bar{j})}(q, \Omega)], \quad (3)$$

where

$$\chi_j = \mathcal{N}_j \left[1 - \frac{\Omega}{2v_F^{(j)}q} \ln \left(\frac{\Omega + v_F^{(j)}q}{\Omega - v_F^{(j)}q} \right) \right] \quad (4)$$

with $\mathcal{N}_j = v_F^{(j)} m_j^2 / 2\pi^2$ being the density of states of each component per unit volume at the Fermi level. In writing these equations we have specifically assumed that we are treating the case of long-wavelength excitations propagating with wave number q along the axis of an elongated cylindrical trap, with the Fourier transform $\delta V^{(j)}(q, \Omega)$ of the driving potentials being independent of the radial coordinate and the Fourier transform $\delta n^{(j)}(q, \Omega)$ of the density distortions being taken at the value $r = 0$ of the radial coordinate. Following [9] and [15] it is easily seen that the collective modes of the Fermi gas described by Eq. (3) are determined by the solutions of the equation

$$1 - g^2 \chi_1(q, \Omega) \chi_2(q, \Omega) = 0, \quad (5)$$

yielding in general two eigenfrequencies $\Omega_j(q)$.

Let us turn next to the calculation of the Fermi velocities. Each of them is determined by the corresponding single-particle dispersion relation as $v_F = \partial E(k) / \partial k|_{k=k_F}$, yielding in a local density approximation

$$v_F^{(j)} = (2\mu_{\text{loc}}^{(j)} / m_j)^{1/2} \quad (6)$$

where $\mu_{\text{loc}}^{(j)}(\mathbf{r}) = \mu^{(j)} - U^{(j)}(\mathbf{r})$ is the local chemical potential. In cylindrical harmonic confinement and in the absence of interactions $v_F^{(j)}$ can be written as

$$v_F^{(j)}(r, z) = \left[2 \left(\mu^{(j)} - V^{(j)}(r, z) \right) / m_j \right]^{1/2} \quad (7)$$

where $V^{(j)}(r, z) = m_j \omega_j^2 (r^2 + \varepsilon_j^2 z^2) / 2$, with radial trap frequency ω_j and anisotropy ε_j . Under driving the radial and axial components of $v_F^{(j)}$ then obey harmonic equations of motion,

$$v_F^{(j)}(t)|_{z=0} = \left(2\mu^{(j)} / m_j \right)^{1/2} \sin(\omega_j t + \phi_r) \quad (8)$$

and

$$v_F^{(j)}(t)|_{r=0} = \left(2\mu^{(j)} / m_j \right)^{1/2} \sin(\varepsilon_j \omega_j t + \phi_z), \quad (9)$$

where the phases ϕ_r and ϕ_z are determined by the initial value of the perturbation. In the presence of mean-field interactions, on the other hand, Eq. (7) is replaced by

$$v_F^{(j)}(r, z) = \left[2 \left(\mu^{(j)} - V^{(j)}(r, z) - g n_0^{(\bar{j})}(r, z) \right) / m_j \right]^{1/2}. \quad (10)$$

In this case harmonicity under driving will be lost, except when the mean field term can be treated perturbatively and for small axial displacements from to

the center of the trap. In this regime it is easy to demonstrate that the mean-field interactions lower the Fermi velocity. More generally, their net effect is to decrease the chemical potential by inducing a decrease of the fermion density.

With the above as background, we conclude this section by presenting our estimates for the speed c_0 of collisionless sound waves propagating along the trap axis at $r = 0$ in two special cases, that will be tested in the next section by comparison with the evolution of density profiles in time from the numerical solution of Eq. (1):

(i) *A single-component Fermi gas.* Setting $g = 0$, Eqs. (3) and (4) immediately yield

$$c_0 = v_F(0, z). \quad (11)$$

This situation will arise not only in the obvious case where the interspecies mean-field interactions vanish, but also in the case where they become so strong in a two-component Fermi gas that the regime of phase separation predicted by the theory [13] is being approached. In this latter case the residual mean-field interactions with the second species merely shift the chemical potential of the species that resides in the inner part of the trap and hence will shift its Fermi velocity.

(ii) *A symmetric two-component Fermi gas.* Taking equal masses and numbers of particles for the two fermionic species inside identical traps, we can write $c_0 = \lambda v_F$ for the local speed of sound wave propagation and determine λ from Eq. (5) using the Landau Fermi-liquid theory to describe the mean-field interactions through the appropriate Landau parameters. Only the spin up-down scattering is allowed in the s -wave channel for a two-component mixture of spin polarized fermions, so that the only non-zero interaction parameters are F_0^s and F_0^a with the condition $F_0^s = -F_0^a$ ($= F_0$, say). Equation (5) can be written in the form

$$\frac{\lambda}{2} \ln \left(\frac{\lambda + 1}{\lambda - 1} \right) = 1 + \frac{1}{F_0} \quad (12)$$

with

$$F_0 = g\mathcal{N} = 2ak_F/\pi. \quad (13)$$

In Figure 1 we have plotted the behaviour of the solution of Eq. (12) as a function of the Fermi velocity for various values of the scattering length. We also show in Figure 2 the values of v_F and c_0 as functions of the scattering length, for the choice of the other system parameters that will be adopted in the numerical calculations reported in the next section. It is seen from these figures that, in order to obtain a very significant increase of the speed of zero sound over the Fermi velocity from repulsive mean-field interactions, one would need to work on a high-density system having huge values of the scattering length. The value of a can to some extent be tuned by exploiting

Feshbach resonances [16], but strong repulsions will also favour demixing of the two-component Fermi gas.

3 Numerical results

3.1 Perturbation introduced by a permanent laser beam

As a first case we consider a one-component gas of 1000 spin-polarized ^{40}K atoms inside an axially symmetric trap with $\omega = 100 \text{ s}^{-1}$ and $\varepsilon = 0.1$. We use 200 computational particles to represent each fermion, in order to obtain a low noise-to-signal ratio [3]. The equilibrium density profile is perturbed by an effective potential $U_0 \exp(-z^2/2\sigma^2)$ with amplitude U_0 and width σ , which simulates a laser beam acting continuously on the centre of the trap. The fermions interacting with the laser are pushed out of the trap centre and the density distortion moves towards the ends of the trap with a velocity which corresponds to the local Fermi velocity given by Eq. (7). Figure 3 shows the evolution in time of the perturbation along the z axis for $r = 0$. For such a system the maximum value of the axial zero-sound velocity, which is equal to the axial Fermi velocity, can be evaluated using Eq. (7) as $c_0^{max}|_{r=0} = v_F^{max}|_{r=0} = 0.383 a_{ho}/ms$, where $a_{ho} = (\hbar/m\omega)^{1/2}$ is the radial harmonic oscillator length. Figure 3 also shows that the positions of the density peaks as calculated numerically at various time steps are in good agreement with those estimated from Eq. (7).

We consider next a 50-50 mixture of 2000 ^{40}K atoms which are polarized in the $7/2$ and $9/2$ spin states, under the same external potentials as in the previous case. The value of the scattering length of ^{40}K ($a = 80$ Bohr radii a_0) is so small that v_F is lowered by the interactions by only 0.1%. From Fig. 2 it is evident that the speed of zero sound is practically unchanged. To see the interaction effects we study the case $a = 2 \times 10^4 a_0$. For this value of the scattering length the Fermi velocity is obtained from the numerical calculation of the chemical potential and of the effective potential as $v_F^{max}|_{r=0} = 0.343 a_{ho}/ms$. The corresponding values of λ and c_0 are 1.01 and $0.347 a_{ho}/ms$ respectively (see Fig. 2). The time evolution of the perturbation in the two components of the interacting Fermi gas is shown in Fig. 4, in comparison with that of the noninteracting gas.

At still higher couplings spatial phase separation starts in the two-component Fermi gas. The case $a = 8 \times 10^4 a_0$ is illustrated in Figure 5. The two components are almost completely demixed and only one of them feels the external perturbation. In this case the interactions with the second component merely shift the chemical potential entering the evaluation of the Fermi velocity of

the first component, which equals the speed of propagation of zero sound.

3.2 Perturbation introduced by a compressed slow light pulse

In the work of Dutton *et al.* [12] ultra-compressed slow light-pulses were used to pump a small slice of a Bose-Einstein condensate into an untrapped state, leaving behind a sharp hole in the density profile. The density defect in the condensate evolves through the formation of solitons, this process being analogous to the creation of shock waves in a classical fluid.

We generate the same type of initial profile in a two-component Fermi gas for various shapes of the density vacancy (V-shape or U-shape of various sizes) and examine the effects of the density gradient and of the size of the defect. No coherent behaviour is observed in the time evolution of the density profiles. In Fig. 6 we plot the time evolution of one of the two components of the Fermi gas for various values of the scattering length ($a = 0, 800 a_0$ and $2 \times 10^4 a_0$) in the case of a small U-shape vacancy. In the two former cases the particles in filling the vacancy generate some density waves, which reach a maximum amplitude after about 150 ms. This is the time lag needed for the perturbation to arrive at the ends of the trap and to be reflected there, as can be roughly estimated by dividing the axial half-length L_z of the trap by c_0^{max} giving $L_z/c_0^{max} \simeq 140$ ms. Because of the absence of thermal dissipation in our model, the density waves continue to travel along the profile and are again reflected at the ends of the trap with a periodicity of about $2L_z/c_0^{max} \simeq 280$ ms. The revivals of smaller amplitude which are seen to occur at about 300 ms correspond to the situation in which the perturbation is passing through the centre of the trap. On increasing the coupling strength up to $a = 2 \times 10^4 a_0$ (right panel in Fig. 6), we find that the restoring force due to the other fermionic component plays a role in depressing the intensity of the density waves relative to those seen in the weak-coupling regime.

4 Conclusions

In summary, we have studied the propagation of collisionless sound waves in a trapped two-component Fermi gas, assuming a mean-field model for the repulsive interactions between the two fermionic species and neglecting dissipative collisions as described by a Boltzmann quantum collision integral. The inclusion of such collisions is needed to examine the transition from the zero-sound to the first-sound regime [3], that we expect will be characterized by a marked change in the speed of sound propagation. We also expect that zero-sound waves will be Landau-damped in the case of attractive interactions, as is the

case for a homogeneous Fermi liquid [6].

We have found that, both at weak coupling and in the strong-coupling regime where the two Fermi clouds are demixing from their mutual repulsions, the speed of zero-sound waves is very close to the Fermi velocity as determined by the local particle density through the local chemical potential. These results have been obtained from comparing semi-analytical estimates with numerical studies of the evolution of peaks in the density profiles under driving from an external potential simulating a blue-detuned laser that keeps expelling atoms from the central region of the trap.

We have also examined numerically the time evolution of impulsively created density defects which are characterized by sharp density gradients in a two-component Fermi gas with repulsive interactions. In the collisionless regime we have found that the filling of the vacancy at the trap centre generates density waves which travel to the ends of the trap and are back-reflected there, so that they appear as periodic revivals of distortions in the density profile. These revivals become attenuated as the strength of the coupling is increased, presumably as a consequence of the increasing efficiency of momentum-redistribution processes through non-dissipative collisions at strong coupling.

Acknowledgements

We acknowledge support from INFM through PRA2001-Photonmatter. ZA also acknowledges support from TUBITAK and from the Research Fund of the University of Istanbul under Project Number BYP-110/12122002.

References

- [1] S.D. Gensemer and D.S. Jin, *Phys. Rev. Lett.* **87** (2001) 173201.
- [2] B. DeMarco and D.S. Jin, *Phys. Rev. Lett.* **88** (2002) 040405.
- [3] F. Toschi, P. Vignolo, S. Succi, and M.P. Tosi, *cond-mat/0210577*.
- [4] M.R. Andrews, D.M. Kurn, H.-J. Miesner, D.S. Durfee, C.G. Townsend, S. Inouye, and W. Ketterle, *Phys. Rev. Lett.* **79** (1997) 553.
- [5] W.R. Abel, A.C. Anderson, and J.C. Wheatley, *Phys. Rev. Lett.* **17** (1966) 74.
- [6] D. Pines and P. Nozières, *The Theory of Quantum Liquids* (Benjamin, New York, 1966).

- [7] K. Sköld, C.A. Pelizzari, R. Kleb, and C.E. Ostrowski, Phys. Rev. Lett. **37** (1976) 842.
- [8] C.H. Aldrich III, C.J. Pethick, and D. Pines, Phys. Rev. Lett. **37** (1976) 845.
- [9] S.K. Yip and T.L. Ho, Phys. Rev. A **59** (1999) 4653.
- [10] B. Damski, K. Sacha, and J. Zakrzewski, J. Phys. B **35** (2002) L153.
- [11] M. Rodriguez and P. Törmä, Phys. Rev. A **66** (2002) 033601.
- [12] Z. Dutton, M. Budde, C. Slowe, and L.V. Hau, Science **293** (2001) 663.
- [13] M. Amoruso, I. Meccoli, A. Minguzzi, and M.P. Tosi, Eur. Phys. J. D **8** (2000) 361.
- [14] A.L. Fetter and J.D. Walecka, *Quantum Theory of Many-Particle Systems* (McGraw Hill, New York, 1971).
- [15] S.K. Yip, Phys. Rev. A **64** (2001) 023609.
- [16] T. Loftus, C.A. Regal, C. Ticknor, J.L. Bohn, and D.S. Jin, Phys. Rev. Lett. **88** (2002) 173201.

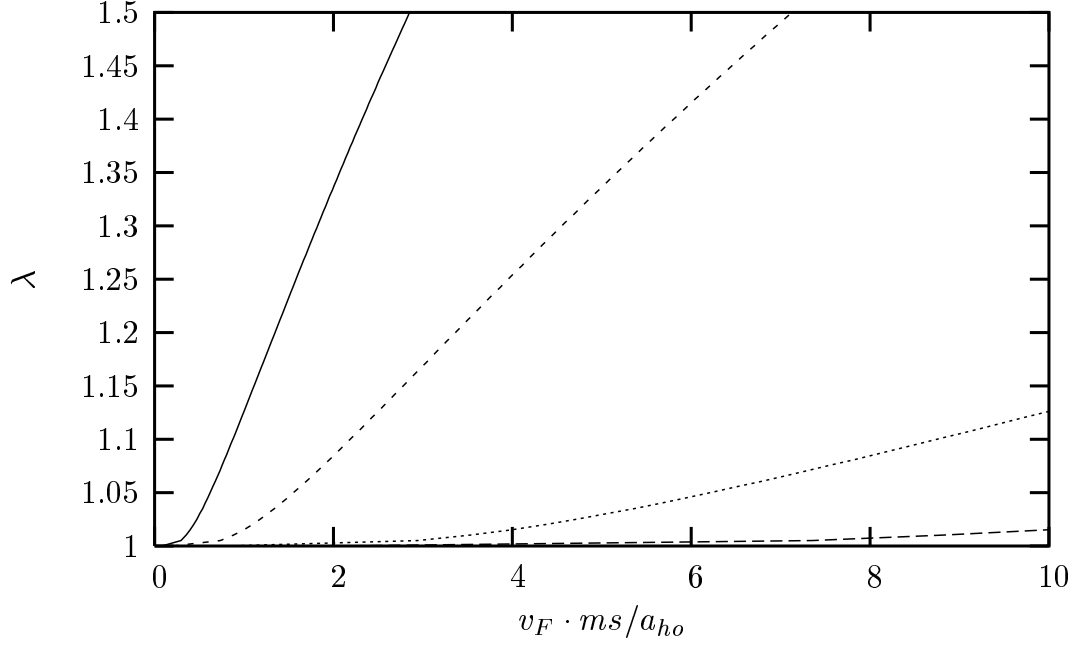


Fig. 1. The λ factor as a function of v_F (in units of a_{ho}/ms with $a_{ho} = (\hbar/m\omega)^{1/2}$) for various values of the scattering length: $a = 2 \times 10^4 a_0$ (continuous line), $8 \times 10^3 a_0$ (short-dashed line), $2 \times 10^3 a_0$ (dotted line) and $800 a_0$ (long-dashed line), a_0 being the Bohr radius.

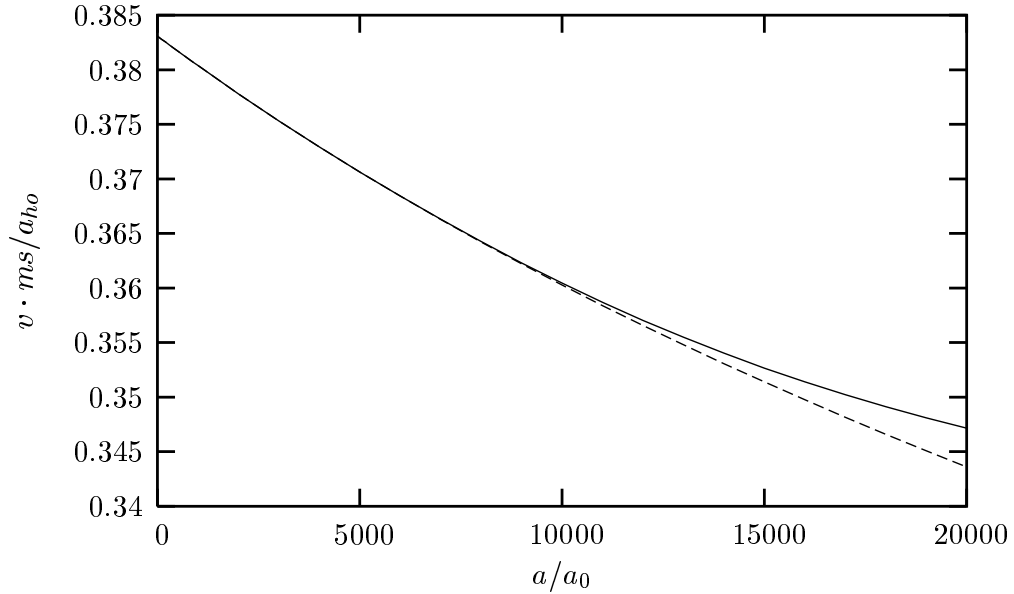


Fig. 2. The speed of zero sound (continuous line) and the Fermi velocity (dashed line), in units of a_{ho}/ms , as functions of the scattering length a (in units of a_0) for a two-component Fermi gas. The calculation refers to 2000 particles in an anisotropic harmonic trap with $\omega = 100 \text{ s}^{-1}$ and $\varepsilon = 0.1$ and the values of the velocities refer to the case of a little perturbation near the centre of the trap.

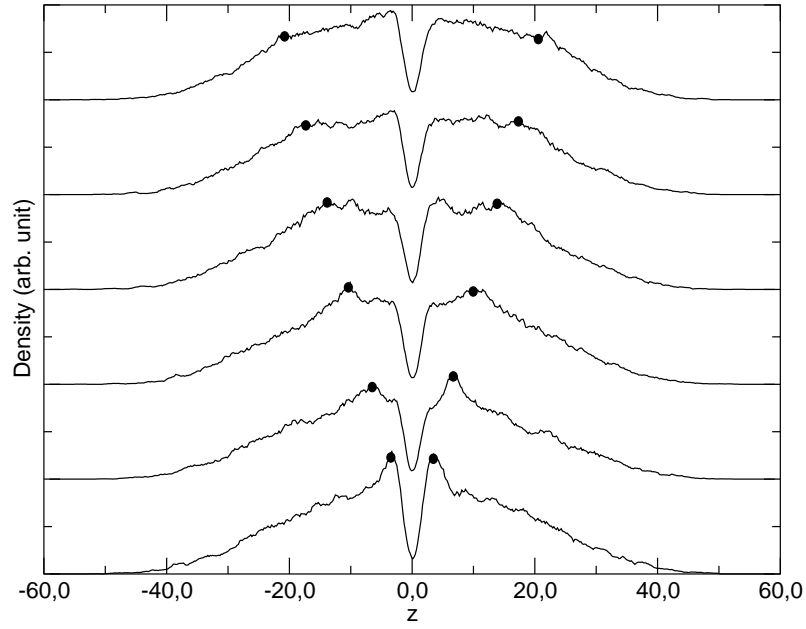


Fig. 3. Time evolution of a defect introduced in a one-component Fermi gas, plotted as a function of the axial distance z (in units of a_{ho}). The bottom profile refers to the initial state and the subsequent profiles are separated by time intervals of 10 ms . The dots indicate the analytical estimate of the position of the perturbation peak from Eq. (7).

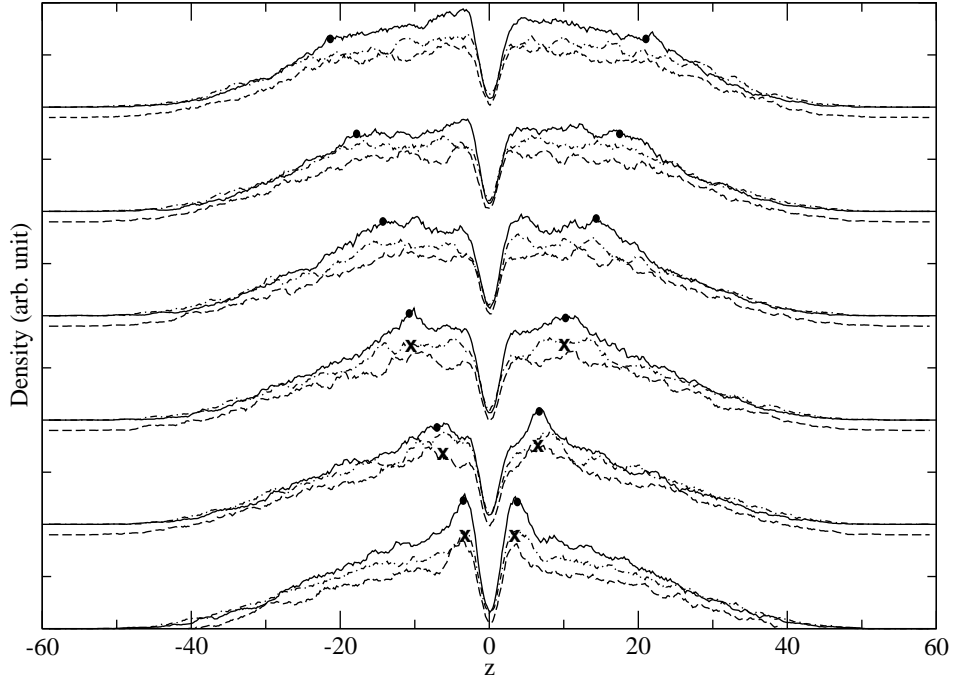


Fig. 4. Time evolution of a defect introduced in both components of an interacting two-component Fermi gas with $a = 2 \times 10^4 a_0$ (dashed lines), in comparison with the one-component case (continuous lines). From bottom to top each profile corresponds to a time lag of 10 ms. Dots indicate the analytical estimate of the position of the peak in the non-interacting case from Eq. (7) and crosses indicate the peak positions corresponding to the zero sound velocity evaluated at $t = 0$ from Eqs. (10), (12) and (13).

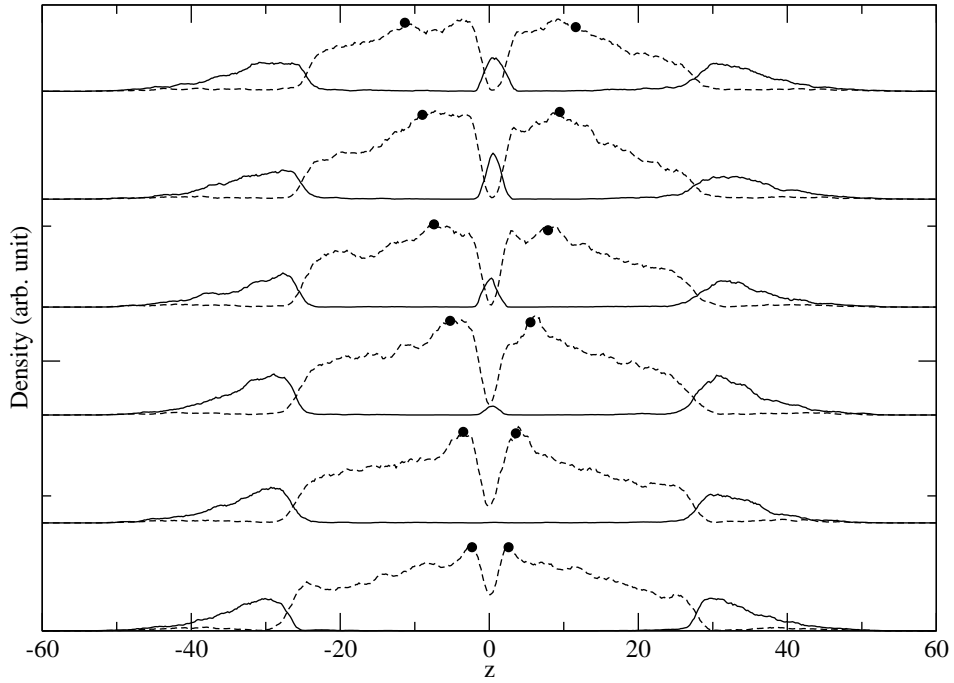


Fig. 5. Time evolution of a defect introduced in one component of an interacting two-component Fermi gas with $a = 8 \times 10^4 a_0$ in a regime of phase separation (dashed lines). From bottom to top each profile corresponds to a time lag of 5 ms. The dots indicate the analytical estimate of the position of the peak of the perturbation from Eq. (7).

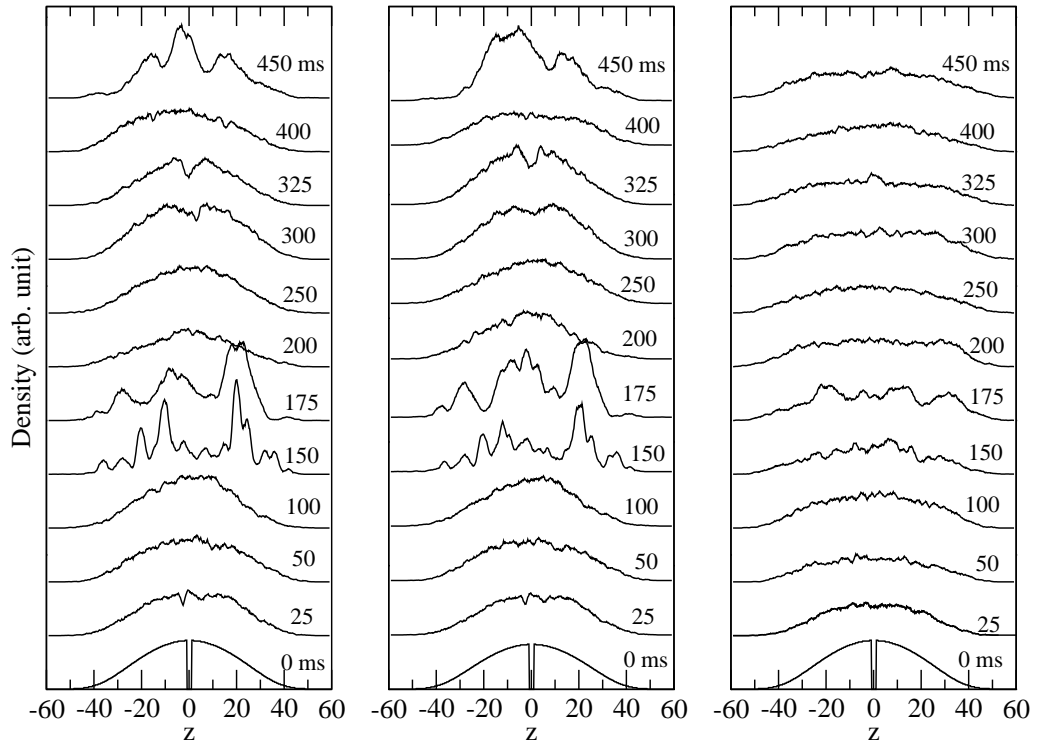


Fig. 6. Time evolution of the axial density profile as a function of z (in units of a_{ho}) for the case of a small U-shape vacancy with $a = 0$, $800 a_0$ and $2 \times 10^4 a_0$ (from left to right). From bottom to top, the time lag of each profile (in ms) is indicated in the figure. The profiles which are not shown in the ranges of time lag between 200 and 300 ms and between 325 and 450 ms are essentially smooth.